Cutaneous Sensory Neurons Expressing the Mrgprd Receptor Sense Extracellular ATP and Are Putative Nociceptors

G. Dussor[1], **M. J. Zylka**[2], **D. J. Anderson**[3], and **E. W. McCleskey**[1]

1*Vollum Institute L474, Oregon Health and Science University, Portland, Oregon*

2*Department of Cell and Molecular Physiology, University of North Carolina Neuroscience Center, University of North Carolina School of Medicine, Chapel Hill, North Carolina*

3*Division of Biology and Howard Hughes Medical Institute, California Institute of Technology, Pasadena, California*

Abstract

Sensory neurons expressing the Mrgprd receptor are known to innervate the outermost living layer of the epidermis, the stratum granulosum. The sensory modality that these neurons signal and the stimulus that they respond to are not established, although immunocytochemical data suggest they could be nonpeptidergic nociceptors. Using patch clamp of dissociated mouse dorsal root ganglion (DRG) neurons, the present study demonstrates that Mrgprd+ neurons have several properties typical of nociceptors: long-duration action potentials, TTX-resistant Na^+ current, and Ca^{2+} currents that are inhibited by mu opioids. Remarkably, Mrgprd+ neurons respond almost exclusively to extracellular ATP with currents similar to homomeric P2X3 receptors. They show little or no sensitivity to other putative nociceptive agonists, including capsaicin, cinnamaldehyde, menthol, pH 6.0, or glutamate. These properties, together with selective innervation of the stratum granulosum, indicate that Mrgprd+ neurons are nociceptors in the outer epidermis and may respond indirectly to external stimuli by detecting ATP release in the skin.

INTRODUCTION

The skin is the largest sensory organ and represents one of the first opportunities for an organism to receive stimuli from the external environment. The exact stimulus varies, but there is an absolute requirement, often for the survival of the organism, that the skin be capable of detecting stimuli in both the innocuous and noxious range. Consequently the skin responds to stimulus intensities ranging from light touch or pleasant warmth to intense piercing or burning pain. The molecular mechanisms by which these sensations are mediated have only partially been uncovered, but recent evidence suggests that keratinocytes, the major cell type in the epidermis, can communicate with sensory neurons in response to certain stimuli (Cook and McCleskey 2002; Koizumi et al. 2004). Thus under some circumstances, the activation of sensory neurons by an external stimulus may be indirect. However, the specific population of sensory neurons that both innervate the epidermis and respond to substances released by keratinocytes has not been identified.

Recently, a family of G-protein-coupled receptors was cloned that showed high expression in sensory neurons of the dorsal root ganglion (DRG) and trigeminal ganglion (TG) (Dong et al. 2001; Lembo et al. 2002). These receptors, named mas-related G-protein-coupled receptors

(Mrgpr, also sensory neuron-specific receptors, SNSR), were found predominantly in small-diameter mouse DRG neurons. One Mrgpr receptor, Mrgprd, was found in the majority of unmyelinated neurons that are labeled by isolectin-B4 (IB4) and express the ATP-gated ion channel P2X3 (Zylka et al. 2003, 2005). Most interestingly, the only innervation target of neurons expressing the Mrgprd receptor is the stratum granulosum of the epidermis (Zylka et al. 2005), one of the four epidermal sublayers and the outermost layer of living cells. Consequently neurons positive for Mrgprd may represent the population of sensory afferents that communicate with keratinocytes in the skin. The sensation that these neurons signal and the signaling molecules that they respond to are important properties that have yet to be conclusively determined.

The experiments in this study have taken advantage of the knock-in mouse line in which all Mrgprd+ neurons express green fluorescent protein (GFP) (Zylka et al. 2005), eliminating the need for retrograde labeling from the skin and allowing the selective study of sensory neurons that innervate the outermost living layer of the epidermis. These data provide functional evidence of a nociceptive phenotype for Mrgprd+ neurons and also uncover a very selective responsiveness to extracellular ATP, a molecule that may be an important signaling mediator between keratinocytes and primary sensory neurons in the epidermis.

METHODS

Animals

All experiments were carried out using protocols approved by the Oregon Health and Science University Institutional Animal Care and Use Committee. Mice (MrgprdΔEGFPf) in which the Mrgprd receptor has been deleted and replaced with a gene for a fluorescent protein, EGFPf, (Zylka et al. 2005) were a generous donation from Dr. David Anderson. Homozygous male mice (−/−) were bred with wild-type C57BL6 females (Charles River) to generate the heterozygous (+/−) mice that were used for all experiments. As the Mrgprd gene is bi-allelic, heterozygous mice express both Mrgprd and EGFP. Mice used in experiments were between 6 and 10 wk of age, and both males and females were used. No differences were observed between male and female mice for any property detailed in this study.

Cell culture

Mice were anesthetized with halothane (4%) and killed by decapitation. The dorsal root ganglia from all available levels were removed and placed in ice-cold Hanks balanced salt solution (divalent free). Ganglia were cut in half and incubated for 20 min in 20 U/ml Papain (Worthington) followed by 15 min in 2 mg/ml Collagenase TypeII (Worthington) and 3 mg/ml Dispase (Roche). Ganglia were then triturated through fire-polished Pasteur pipettes of decreasing diameter and plated on poly-ᴅ-lysine (Becton Dickinson) and laminin (Sigma)-coated plates. After several hours at room temperature to allow adhesion, cells were cultured in a room-temperature, humidified chamber in Liebovitz L-15 medium supplemented with 10% FBS, 10 mM glucose, 5 mM HEPES, 20 ng/ml GDNF (Chemicon), 50 ng/ml NGF (Upstate Cell Signaling Solutions), and 50 U/ml penicillin/streptomycin. Most cells were used within 24 h post plating although some pharmacological experiments using $\alpha\beta$ methylene ATP and TNP-ATP were done within 48 h post plating. No differences were observed between earlier and later time points in these experiments. Additionally, several cultures were used to confirm that GFP+ cells were IB4+ (data not shown).

Electrophysiology

Whole cell patch-clamp experiments were performed on isolated mouse DRG using a MultiClamp 700B (Axon Instruments) patch-clamp amplifier and pClamp 9 acquisition software (Axon Instruments). Recordings were sampled at 5 kHz and filtered at 1 kHz for

ligand-gated channels and 20-kHz sampling/2-kHz filtering for voltage-gated channels (Digidata 1322A, Axon Instruments). Pipettes (OD: 1.5 mm, ID: 0.86 mm, Sutter Instrument) were pulled using a P-87 puller (Sutter Instrument) and heat polished to 2.5−4 MΩ resistance using a microforge (MF-83, Narishige). Series resistance was typically <7 MΩ and was compensated 70−80%. All recordings were performed at room temperature. Input resistance in Table 1 was calculated from the average current size (10 sweeps, 100 ms each) evoked by a step to −70 mV from a holding potential of −60 mV. Cells were visualized using a Nikon DIAPHOT-TMD inverted microscope equipped with a mercury arc lamp for fluorescent excitation. Data were analyzed using Clampfit 9 (Molecular Devices) and Origin 7 (OriginLab). Images in Fig. 1*A* were acquired using Metamorph V6.2r6 and a Zeiss Axiovert 135TV Microscope equipped with a xenon arc lamp for fluorescent excitation and a Princeton Scientific Instruments NTE CCD-512 EBFT camera.

VOLTAGE-GATED CHANNEL RECORDING—Pipette solution used to record Na^+ and Ca^{2+} currents contained (in mM) 120 CsCl, 10 EGTA, 2 $MgCl_2$, 3 NaCl, 40 HEPES, 2 MgATP, and 0.3 Na_2GTP, pH 7.3 (adjusted with *N*-methyl glucamine), and was ~300 mosM. Bath solution contained (in mM) 135 NaCl, 2 $CaCl_2$, 1 $MgCl_2$, 5 KCl, and 10 HEPES, pH 7.4 (adjusted with *N*-methyl glucamine), and was ~330 mosM. External solutions used to record voltage-gated currents were applied during recordings using gravity-fed flow pipes positioned near the cell and controlled by computer-driven solenoid valves. External solution used to record Na^+ currents contained (in mM) 115 TEA-Cl, 20 NaCl, 2 $CaCl_2$, 1 $MgCl_2$, 5 KCl, 10 HEPES, 0.1 $CdCl_2$, and 0.1 $NiCl_2$, pH 7.4 (adjusted with *N*-methyl glucamine), and was ~330 mosM. External solution used to record Ca^{2+} currents contained (in mM) 135 TEA-Cl, 2 $BaCl_2$, 1 $MgCl_2$, 5 KCl, and 10 HEPES, pH 7.4 (adjusted with *N*-methyl glucamine), and was ~330 mosM.

ACTION POTENTIAL AND LIGAND-GATED CHANNEL RECORDING—Pipette solution contained (in mM) 120 KCl, 10 EGTA, 2 $MgCl_2$, 2 NaCl, 40 HEPES, 2 MgATP, and 0.3 Na_2GTP, pH 7.3 (adjusted with *N*-methyl glucamine), and was ~300 mosM. External solution contained (in mM) 135 NaCl, 2 $CaCl_2$, 1 $MgCl_2$, 5 KCl, and 10 HEPES, pH 7.4 (adjusted with *N*-methyl glucamine), and was ~330 mosM. For ligand-gated channels, solutions were rapidly changed during recordings using gravity-fed flow pipes positioned near the cell and controlled by computer driven solenoid valves. The solution exchange time was <20 ms.

Drugs

Tetrodotoxin was from Alomone Labs. Nifedipine, ωConotoxin GVIIA, ωAgatoxin IVA, [D-Ala[2], N-Me-Phe[4], Gly[5]-ol]enkephalin acetate (DAMGO), ATP, $\alpha\beta$ methylene ATP, tri-nitro phenyl ATP (TNP-ATP), cinnamaldehyde, menthol, 1-(m-chlorophenyl) biguanide (mCPBG), nicotine, capsaicin, and glutamic acid were from Sigma. Muscimol was from Sigma-RBI.

Data analysis

Data are expressed as means ± SE. Statistical significance was tested using an unpaired two-tailed Student's *t*-test.

RESULTS

Mrgprd+ neurons exhibit nociceptor-like properties

Patch-clamp electrophysiology was performed on DRG neurons in culture from adult knock-in mice in which GFP is expressed under the control of endogenous Mrgprd regulatory elements. Expression of GFP was used as a marker for cells that contain the Mrgprd receptor (see METHODS). Several cultures were used to confirm that GFP+ cells were also IB4+ (data not

shown) consistent with data from Zylka et al. (2005) showing that all Mrgprd+ cells in native DRG are IB4+. Cells were selected for recording if they were either positive for GFP expression or were similar in diameter to GFP+ neurons but were GFP−. Examples of both Mrgprd+ and Mrgprd− neurons are seen in the phase and corresponding fluorescence image in Fig. 1*A*. The average diameter of both Mrgprd+ and Mrgprd− neurons used (as measured by a calibrated graticule) were similar as were the whole cell capacitance measurements (Table 1). As shown in Fig. 1*B*, both Mrgprd+ and Mrgprd− neurons had long duration action potentials (Table 1) when measured from 0 mV on the rising phase to 0 mV on the falling phase, and they exhibited a shoulder on the falling phase. For comparison, we measured the action potential duration of larger diameter neurons ($42 \pm 3 \mu$m) from the same cultures and found an average duration of 1.9 ± 0.4 ms ($n = 6$, data not shown). Both Mrgprd+ and Mrgprd− neurons also had large action potential overshoots (Table 1). Although the duration of the action potential and the presence of an overshoot are not definitive of the sensory modality of any given neuron, many that signal nociceptive stimuli have been shown to have long-duration action potentials (Djouhri et al. 1998) and have action potentials with overshoots (Djouhri and Lawson 2001).

To determine whether Mrgprd+ neurons displayed voltage-gated Na^+ current resistant to block by tetrodotoxin (TTX), cells were typically held at −90 mV and stepped to more positive potentials in 5-mV increments at 1-s intervals (Fig. 2). Figure 2*A* shows sodium currents (I_{Na}) evoked at the indicated voltages before and after the addition of 1 μM TTX. Subtraction of the TTX-resistant current (TTX-r I_{Na}) from the total (Total I_{Na}) yields the TTX-sensitive current (TTX-s I_{Na}, Fig. 2*B*, ▲, *C*). The peak amplitude of each of the three components is shown at each membrane voltage (Fig. 2*C*). In both Mrgprd+ and Mrgprd− neurons, most of the Na^+ current is resistant to TTX although there is significantly more TTX-r current in Mrgprd + neurons (Table 1). Because TTX-r Na^+ channels are thought to contribute to the duration of the action potential and contribute a large fraction of the depolarizing current during the rising phase (Blair and Bean 2002), this may explain the differences in action potential characteristics (i.e., amplitude, overshoot, and duration) detailed in Table 1. The functional significance of the difference in TTX-r current is unclear but may differentially impact the duration of firing in these populations due to slow inactivation of TTX-r Na^+ channels (Blair and Bean 2003). In any case, these data further suggest that Mrgprd+ neurons are nociceptors given that neurons expressing TTX-r Na^+ current tend to be nociceptive (Djouhri et al. 2003).

Voltage-gated Ca^{2+} current was examined in Mrgprd+ and Mrgprd− neurons for modulation by opioids using the μ-opioid receptor agonist DAMGO. Cells were held at −80 mV and stepped to 0 mV every 20 s and peak amplitudes of I_{Ca} was measured before and after application of 1 μM DAMGO. Cells positive for Mrgprd consistently displayed small inhibition of I_{Ca} (~10%) in response to this concentration of DAMGO (Fig. 3, *A* and *B*) as did cells negative for Mrgprd (not shown). However, almost 90% of Mrgprd+ cells had I_{Ca} that was inhibited by DAMGO. Approximately 60% of Mrgprd- neurons had Ca^{2+} currents inhibited by DAMGO. In all cells tested, the modulation of I_{Ca} was only partially reversible (Fig. 3*B*), but in cells pretreated with the opioid receptor antagonist naloxone (10 μM), no inhibition of Ca^{2+} current was observed (Fig. 3*C*). Given that, in rats, most small-diameter nociceptors are inhibited by opioids and that identified nonnociceptors are not opioid-sensitive (Silbert et al. 2003), these data argue that Mrgprd+ neurons are nociceptors.

Because opioid receptors are thought to modulate several types of Ca^{2+} channels (Rusin and Moises 1995), the expression of different types of voltage-gated Ca^{2+} current was studied in neurons positive and negative for the Mrgprd receptor. Current-voltage plots of I_{Ca}, run from holding potentials of −90 and −50 mV, revealed a prominent shoulder at lower membrane potentials ($\leq$−20 mV) in Mrgprd− neurons (Fig. 4*A*). The peak I_{Ca} at lower potentials in Mrgprd − neurons was sensitive to holding potential with less current produced from a holding potential of −50 mV. As shown in Fig. 4*B*, Mrgprd− neurons had consistently higher I_{Ca} density at −30

mV, and the current at this voltage was blocked, although not completely, by 100 μM Ni^{2+}, suggesting the presence of T-type current in Mrgprd− but not Mrgprd+ neurons. The functional significance of T-type current in Mrgprd− neurons is unclear but may allow the entry of larger amounts of Ca^{2+} during action potentials (McCobb and Beam 1991) and consequently greater neurotransmitter release from these neurons or it may allow these neurons to burst fire action potentials (Lovinger and White 1989; White et al. 1989).

Several different Ca^{2+} current components were revealed at 0 mV after sequential addition of 30 μM nifedipine, 1 μM ω-conotoxin GVIIA, and 250 nM ω-agatoxin IVA (Fig. 4*C*), suggesting the presence of L-type, N-type, and P/Q-type Ca^{2+} channels, respectively. Given that the fraction of ω-conotoxin sensitive (presumably N-type) current is ~15% and this is the most likely high-threshold current inhibited by mu opioids in these neurons (Bourinet et al. 1996), the 10% modulation by DAMGO becomes a large percentage of the current that is available to be inhibited.

Mrgprd+ neurons are highly sensitive to extracellular ATP

To determine the chemical stimuli that Mrgprd+ neurons might respond to, responsiveness to a variety of ligands believed to excite nociceptors was examined in cultured DRG neurons. As can be seen in Fig. 5, 92% of Mrgprd+ neurons responded to application of 50 μM ATP, whereas <30% of Mrgprd− neurons exhibited a response. By contrast, only 5% of Mrgprd+ neurons exhibited currents in response to 1 μM capsaicin, a TRPV1 agonist, compared with about half of Mrgprd− neurons (48%). No more than 15% of Mrgprd+ or Mrgprd− neurons responded to the 5-HT_3 agonist mCPBG (3 μM), pH 6.0, nicotine (500 μm), the TRPA1 agonist cinnamaldehyde (100 μm), the TRPM8 agonist menthol (100 μm), or glutamate (1 mM). Several concentrations of glutamate were applied ranging from 200 μM to 5 mM, and similar results were observed with each concentration. Glutamate induced small currents (typically ≤30 pA) in most Mrgprd+ neurons, but these were usually below the 50 pA value used to score a response as positive. Consistent with prior reports demonstrating that most DRG neuronal cell bodies respond to GABA (Bevan and Winter 1995;Feltz and Rasminsky 1974), all Mrgprd + and Mrgprd− - neurons responded to application of 100 μM muscimol with a $GABA_A$-like current averaging ~600 pA in amplitude (data not shown).

In addition to differences in the fraction of Mrgprd+ and Mrgprd− neurons that respond to ATP, there were also differences in the kinetics of the ATP generated current in the majority of responding neurons. In 95% of Mrgprd+ neurons, the current produced in response to application of either 50 μM ATP or 50 μM $\alpha\beta$Me-ATP was fast activating and rapidly desensitizing (Fig. 6*A*). Both the pharmacology and the current kinetics suggest the presence of homomeric P2X3 receptors (Chen et al. 1995;Grubb and Evans 1999;North and Surprenant 2000;Pankratov Yu et al. 2001). In Mrgprd− neurons, 65% of those responding to either 50 μM ATP or 50 μM $\alpha\beta$Me-ATP displayed current that had more prolonged kinetics and was much slower to desensitize (Fig. 6*B*), suggesting the presence of P2X2/3 heteromeric channels. The remaining 5% of Mrgprd+ neurons had current similar to that generated by P2X2/3 heteromeric channels, and the remaining 35% of Mrgprd− neurons had P2X3-like current. The peak current density in response to ATP was not different between Mrgprd+ and Mrgprd− neurons (40 pA/pF, data not shown).

Because application of P2X3 agonists produce rapidly desensitizing current that can take several minutes or longer to fully recover (Pratt et al. 2005; Sokolova et al. 2004), a protocol was used in which $\alpha\beta$Me-ATP was applied every 60 s to study the P2X3-like current at the same time point on its recovery from desensitization (Fig. 6*C*). This allowed reproducibly sized currents to be generated at regular intervals so that antagonist block could be examined. The current produced in Mrgprd+ neurons in response to application of 50 μM $\alpha\beta$Me-ATP at 60-s intervals was blocked by pre- and co-application of the mixed P2X1, P2X3, and P2X2/3

antagonist TNP-ATP (50 nM) (North and Surprenant 2000), supporting the hypothesis that current is mediated by P2X3. After washout of TNP-ATP, the next application of $\alpha\beta$Me-ATP produced larger current than the previous applications likely because the channels were not activated during TNP-ATP block, thus allowing the channels more time for recovery from desensitization (i.e., 120 vs. 60 s).

DISCUSSION

These data show that mouse sensory neurons that express the Mrgprd receptor have classic properties of unmyelinated nociceptors: small-diameter cell bodies, long-duration action potentials, TTX-resistant Na^+ currents, and Ca^{2+} currents inhibited by opioids. Unlike other small sensory neurons, nearly all Mrgprd+ neurons fail to respond to capsaicin, acid, and menthol yet uniformly exhibit currents evoked by extracellular ATP. These results suggest two conclusions: the sensory neurons that innervate the outermost layer of mouse skin are nociceptors and they are specialized to detect extracellular ATP. Strict dependence on ATP implies that the neurons themselves are not the primary sensor of local noxious events. Rather skin cells, such as keratinocytes, must sense the event and release the ATP.

Although the data presented here demonstrate that Mrgprd+ neurons display "nociceptor-like" properties, they cannot conclusively determine that these neurons are nociceptors. Because it is not yet known whether nonnoxious stimuli can cause the release of ATP from keratinocytes, these neurons may sense other stimuli. However, recent evidence using an *ex vivo* preparation supports the conclusions presented here by demonstrating that these neurons are polymodal nociceptors (Lawson et al. 2007). This finding is intriguing because it suggests that there may be more than one type of stimulus that can initiate signaling between keratinocytes and sensory neurons using ATP. Recent reports have demonstrated that both mechanical stimulation and cell damage can cause the release of ATP from keratinocytes (Cook and McCleskey 2002; Koizumi et al. 2004). The released ATP was shown to activate P2 receptors on neighboring DRG neurons in culture. Keratinocytes can also respond to changes in temperature as they express temperature-sensitive TRP channels (Lee and Caterina 2005; Lumpkin and Caterina 2007). However, it is unknown at this point whether keratinocytes actually release ATP in response to changes in temperature. Also unknown is whether keratinocytes and sensory neurons can in fact communicate in vivo, but they are known to be in direct contact (Chateau and Misery 2004), which provides anatomical support for this concept.

What is surprising about the results presented here is that most Mrgprd+ neurons did not respond with ionic currents to ligands other than ATP. The ATP sensitivity of the Mrgprd+ population corresponds well with histological data demonstrating that all Mrgprd+ neurons express the P2X3 receptor (Zylka et al. 2005). What the present data show is that this population appears to be selectively excited by ATP through this single ATP-gated channel. Although all Mrgprd+ neurons did respond to the GABA agonist muscimol, and GABA synthesis may occur in fibroblasts in the epidermis (Ito et al. 2007), it is unclear whether GABA can be released in the epidermis. So GABA receptors may not participate in peripheral activation of these neurons but may be involved in central modulation. Additionally, we did not examine responsiveness to the proposed ligand for Mrgprd, β-alanine (Shinohara et al. 2004). If this ligand is present in the skin, it would represent an additional stimulus that Mrgprd+ neurons are capable of detecting. Based on the lack of response to the other ligands tested, direct sensation of temperature through TRPV1 and TRPM8 or the presence of chemical mediators of pain appear not to be important for Mrgprd+ neurons. The reasons for this are unclear, but because Mrgprd + fibers make up 60% of epidermal innervation (Zylka et al. 2005), it may be left to the other 40% of epidermal afferents that terminate in deeper epidermal layers to sense these stimuli. Further, Zylka et al. found that 10% of Mrgprd-containing fibers were intertwined with CGRP-

containing fibers. The functional significance of this is unknown, but it may allow the nervous system to respond to stimuli in the stratum granulosum that Mrgprd+ neurons cannot detect.

Additionally, ATP may not be the only substance released from keratinocytes that Mrgprd+ neurons are capable of detecting. A recent study detailed the ability of CB_2 cannabinoid receptor agonists to produce antinociception by causing the release of β-endorphin from keratinocytes in the stratum granulosum of the epidermis (Ibrahim et al. 2005). A similar study showed that activation of the ET_B endothelin receptor, which is present on keratinocytes in both the stratum granulosum and stratum spinosum, can also cause the release of β-endorphin from keratinocytes producing antinociception (Khodorova et al. 2003). Because Mrgprd+ neurons are the majority of the innervation of the stratum granulosum (Zylka et al. 2005), these neurons may be responsive to β-endorphin released from keratinocytes; this may explain the high percentage of opioid-sensitive Mrgprd+ neurons. Thus keratinocytes may be capable of both stimulating and inhibiting the activity of cutaneous afferents using ATP and β-endorphin, respectively. Future studies will determine whether activators of other G-protein-coupled receptors in addition to μ-opioid agonists, which might also be released in the skin, can modulate the activity of these neurons. Ultimately it may be the case that for certain sensations keratinocytes are the actual "sensors" in the skin and sensory neurons merely relay the signal by responding to one or more mediators released by keratinocytes (Denda et al. 2007; Lumpkin and Caterina 2007).

Labeling for Mrgprd allows the in vitro study of sensory neurons the target innervation of which, the stratum granulosum of the epidermis, is clearly defined. Using this method, the experiments described here and those performed previously have only begun to uncover properties of these cutaneous afferents that are some of the closest neuronal terminals to the outside world. It may not be surprising if their phenotype is in fact nociceptive as responses to potentially damaging stimuli would be initiated before any other. These data show that Mrgprd + neurons are activated selectively by the presence of ATP. This suggests that an intermediate (i.e., keratinocytes) may initiate signaling into the CNS by releasing ATP onto Mrgprd+ nociceptors. Although it is possible that dependence on an intermediate can slow down the initiation of signaling, this may be outweighed by the additional level of stimulus filtering provided by the intermediate. This filtering ensures that stimuli that produce a response are those that are truly capable of causing damage, a determination made by the epidermis itself and not the nervous system.

REFERENCES

Bevan S, Winter J. Nerve growth factor (NGF) differentially regulates the chemosensitivity of adult rat cultured sensory neurons. J Neurosci 1995;15:4918–4926. [PubMed: 7623122]

Blair NT, Bean BP. Roles of tetrodotoxin (TTX)-sensitive Na^+ current, TTX-resistant Na^+ current, and Ca^{2+} current in the action potentials of nociceptive sensory neurons. J Neurosci 2002;22:10277–10290. [PubMed: 12451128]

Blair NT, Bean BP. Role of tetrodotoxin-resistant Na^+ current slow inactivation in adaptation of action potential firing in small-diameter dorsal root ganglion neurons. J Neurosci 2003;23:10338–10350. [PubMed: 14614093]

Bourinet E, Soong TW, Stea A, Snutch TP. Determinants of the G protein-dependent opioid modulation of neuronal calcium channels. Proc Natl Acad Sci USA 1996;93:1486–1491. [PubMed: 8643659]

Chateau Y, Misery L. Connections between nerve endings and epidermal cells: are they synapses? Exp Dermatol 2004;13:2–4. [PubMed: 15009109]

Chen CC, Akopian AN, Sivilotti L, Colquhoun D, Burnstock G, Wood JN. A P2X purinoceptor expressed by a subset of sensory neurons. Nature 1995;377:428–431. [PubMed: 7566119]

Cook SP, McCleskey EW. Cell damage excites nociceptors through release of cytosolic ATP. Pain 2002;95:41–47. [PubMed: 11790466]

Denda M, Nakatani M, Ikeyama K, Tsutsumi M, Denda S. Epidermal keratinocytes as the forefront of the sensory system. Exp Dermatol 2007;16:157–161. [PubMed: 17286806]

Djouhri L, Bleazard L, Lawson SN. Association of somatic action potential shape with sensory receptive properties in guinea-pig dorsal root ganglion neurones. J Physiol 1998;513:857–872. [PubMed: 9824723]

Djouhri L, Fang X, Okuse K, Wood JN, Berry CM, Lawson SN. The TTX-resistant sodium channel Nav1.8 (SNS/PN3): expression and correlation with membrane properties in rat nociceptive primary afferent neurons. J Physiol 2003;550:739–752. [PubMed: 12794175]

Djouhri L, Lawson SN. Differences in the size of the somatic action potential overshoot between nociceptive and non-nociceptive dorsal root ganglion neurones in the guinea pig. Neuroscience 2001;108:479–491. [PubMed: 11738261]

Dong X, Han S, Zylka MJ, Simon MI, Anderson DJ. A diverse family of GPCRs expressed in specific subsets of nociceptive sensory neurons. Cell 2001;106:619–632. [PubMed: 11551509]

Feltz P, Rasminsky M. A model for the mode of action of GABA on primary afferent terminals: depolarizing effects of GABA applied iontophoretically to neurones of mammalian dorsal root ganglia. Neuropharmacology 1974;13:553–563. [PubMed: 4153679]

Grubb BD, Evans RJ. Characterization of cultured dorsal root ganglion neuron P2X receptors. Eur J Neurosci 1999;11:149–154. [PubMed: 9987019]

Ibrahim MM, Porreca F, Lai J, Albrecht PJ, Rice FL, Khodorova A, Davar G, Makriyannis A, Vanderah TW, Mata HP, Malan TP Jr. CB2 cannabinoid receptor activation produces antinociception by stimulating peripheral release of endogenous opioids. Proc Natl Acad Sci USA 2005;102:3093–3098. [PubMed: 15705714]

Ito K, Tanaka K, Nishibe Y, Hasegawa J, Ueno H. GABA-synthesizing enzyme, GAD67, from dermal fibroblasts: evidence for a new skin function. Biochim Biophys Acta 2007;1770:291–296. [PubMed: 17113713]

Khodorova A, Navarro B, Jouaville LS, Murphy JE, Rice FL, Mazurkiewicz JE, Long-Woodward D, Stoffel M, Strichartz GR, Yukhananov R, Davar G. Endothelin-B receptor activation triggers an endogenous analgesic cascade at sites of peripheral injury. Nat Med 2003;9:1055–1061. [PubMed: 12847519]

Koizumi S, Fujishita K, Inoue K, Shigemoto-Mogami Y, Tsuda M, Inoue K. Ca^{2+} waves in keratinocytes are transmitted to sensory neurons: the involvement of extracellular ATP and P2Y2 receptor activation. Biochem J 2004;380:329–338. [PubMed: 14967069]

Lawson JJ, McIlwrath SL, Zylka MJ, Anderson DJ, Koerber HR. The g-protein coupled receptor mrgprd is found in a specific subset of cutaneous nociceptors. Soc Neurosci Abstract 2007;509.14

Lee H, Caterina MJ. TRPV channels as thermosensory receptors in epithelial cells. Pfluegers 2005;451:160–167.

Lembo PM, Grazzini E, Groblewski T, O'Donnell D, Roy MO, Zhang J, Hoffert C, Cao J, Schmidt R, Pelletier M, Labarre M, Gosselin M, Fortin Y, Banville D, Shen SH, Strom P, Payza K, Dray A, Walker P, Ahmad S. Proenkephalin A gene products activate a new family of sensory neuron–specific GPCRs. Nat Neurosci 2002;5:201–209. [PubMed: 11850634]

Lovinger DM, White G. Post-natal development of burst firing behavior and the low-threshold transient calcium current examined using freshly isolated neurons from rat dorsal root ganglia. Neurosci Lett 1989;102:50–57. [PubMed: 2779845]

Lumpkin EA, Caterina MJ. Mechanisms of sensory transduction in the skin. Nature 2007;445:858–865. [PubMed: 17314972]

McCobb DP, Beam KG. Action potential waveform voltage-clamp commands reveal striking differences in calcium entry via low- and high voltage-activated calcium channels. Neuron 1991;7:119–127. [PubMed: 1648936]

North RA, Surprenant A. Pharmacology of cloned P2X receptors. Annu Rev Pharmacol Toxicol 2000;40:563–580. [PubMed: 10836147]

Pankratov Yu V, Lalo UV, Dashkin AN, Krishtal A. Heterogeneity of the functional expression of P2X3 and P2X2/3 receptors in the primary nociceptive neurons of rat. Neurochem Res 2001;26:993–1000. [PubMed: 11699951]

Pratt EB, Brink TS, Bergson P, Voigt MM, Cook SP. Use-dependent inhibition of P2X3 receptors by nanomolar agonist. J Neurosci 2005;25:7359–7365. [PubMed: 16093386]

Rusin KI, Moises HC. mu-Opioid receptor activation reduces multiple components of high-threshold calcium current in rat sensory neurons. J Neurosci 1995;15:4315–4327. [PubMed: 7540671]

Shinohara T, Harada M, Ogi K, Maruyama M, Fujii R, Tanaka H, Fukusumi S, Komatsu H, Hosoya M, Noguchi Y, Watanabe T, Moriya T, Itoh Y, Hinuma S. Identification of a G-protein-coupled receptor specifically responsive to beta-alanine J Biol Chem 2004;279:23559–23564.

Silbert SC, Beacham DW, McCleskey EW. Quantitative single-cell differences in mu-opioid receptor mRNA distinguish myelinated and unmyelinated nociceptors. J Neurosci 2003;23:34–42. [PubMed: 12514199]

Sokolova E, Skorinkin A, Fabbretti E, Masten L, Nistri A, Giniatullin R. Agonist-dependence of recovery from desensitization of P2X(3) receptors provides a novel and sensitive approach for their rapid up or downregulation. Br J Pharmacol 2004;141:1048–1058. [PubMed: 14980981]

White G, Lovinger DM, Weight FF. Transient low-threshold Ca^{2+} current triggers burst firing through an afterdepolarizing potential in an adult mammalian neuron. Proc Natl Acad Sci USA 1989;86:6802–6806. [PubMed: 2549548]

Zylka MJ, Dong X, Southwell AL, Anderson DJ. Atypical expansion in mice of the sensory neuron-specific Mrg G-protein-coupled receptor family. Proc Natl Acad Sci USA 2003;100:10043–10048. [PubMed: 12909716]

Zylka MJ, Rice FL, Anderson DJ. Topographically distinct epidermal nociceptive circuits revealed by axonal tracers targeted to Mrgprd. Neuron 2005;45:17–25. [PubMed: 15629699]
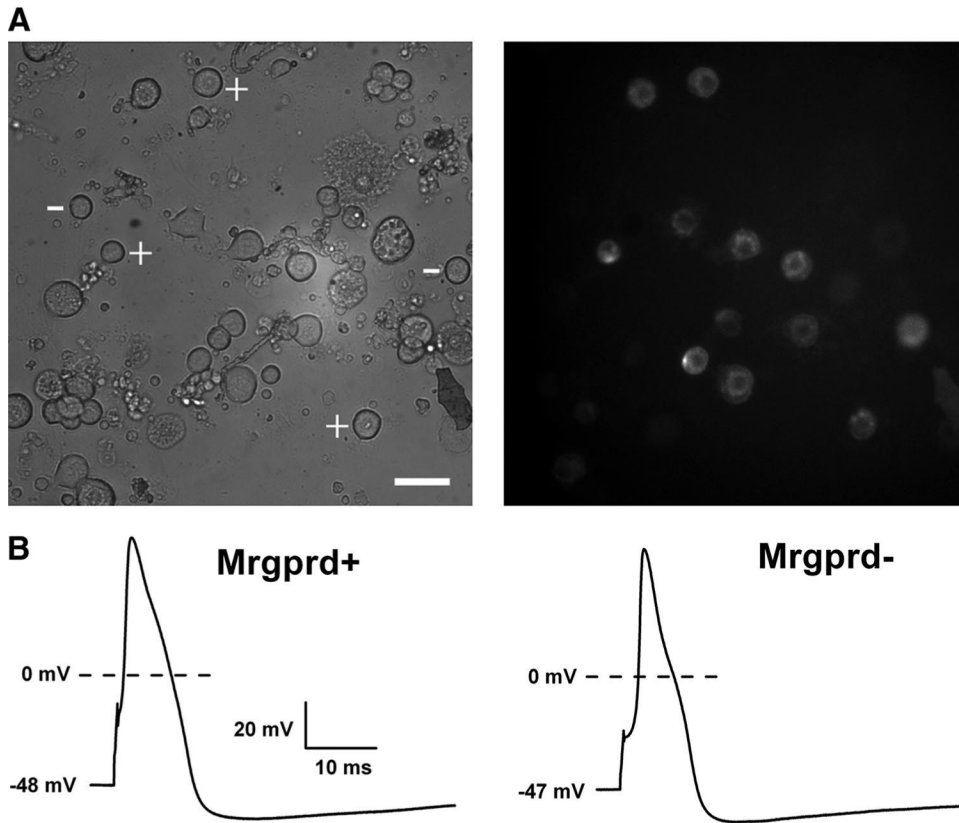
FIG. 1.
Mrgprd+ dorsal root ganglion (DRG) neurons are small diameter and have long-duration action potentials. *A*: phase (*left*) and fluorescence (*right*) images show the size of isolated DRG neurons. Neurons were selected as positive (marked +) if clear expression of green fluorescent protein (GFP) was visualized after fluorescent excitation. Neurons were selected as negative (marked −) if no GFP could be observed after fluorescent excitation. Not all visible Mrgprd+ and Mrgprd− neurons are marked in the phase image on the *left* and Mrgprd− neurons the size of which was markedly larger or smaller than Mrgprd+ neurons were not used in this study. Scale bar, 40 μm. *B*: action potentials evoked in an Mrgprd+ neuron (*left*) and an Mrgprd− neuron (*right*)in response to a 2-nA current injection for 0.5 ms. Note the long duration (measured at 0 mV) and prominent shoulder on the falling phase in both Mrgprd+ and Mrgprd − neurons.
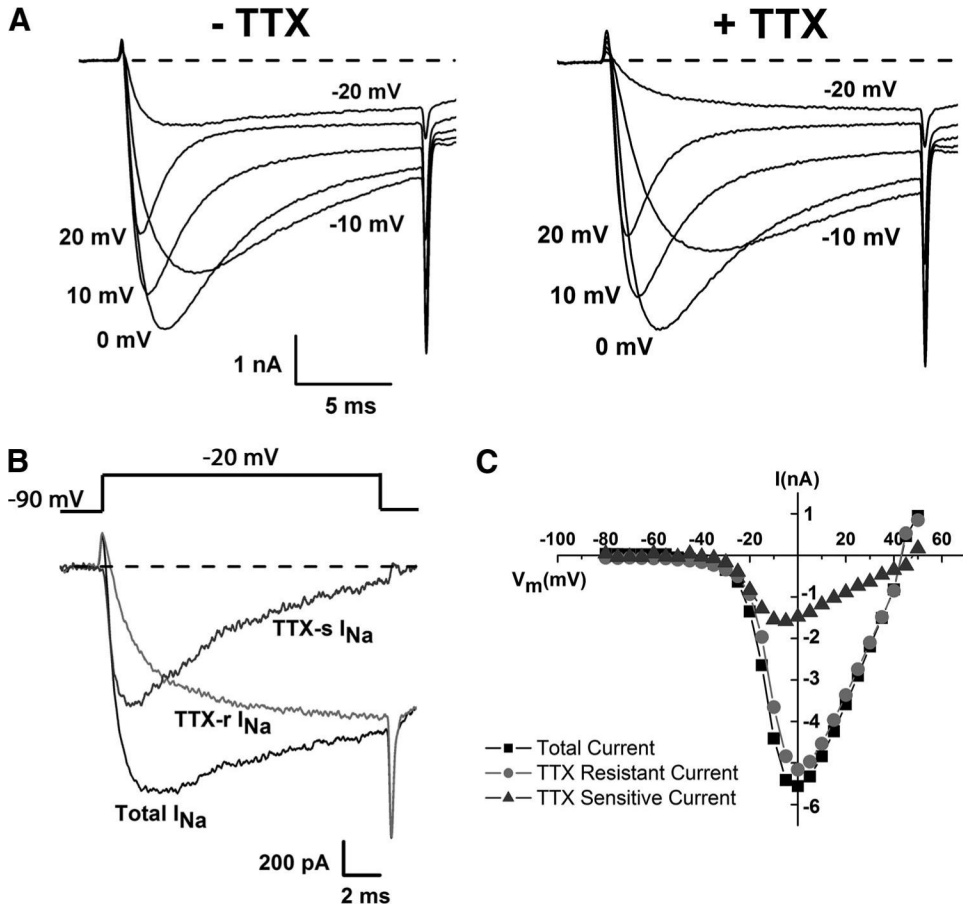
FIG. 2.
Mrgprd+ neurons display prominent TTX-resistant voltage-gated Na$^+$ current. *A*: Na$^+$ current evoked in a representative Mrgprd+ neuron by steps from a holding potential of −90 mV to the indicated test potentials before (*left*) and after (*right*) application of 1 μM TTX. Sweeps were selected from the protocol used to generate *C* and steps were given every 1 s. *B*: Na$^+$ current components in the same Mrgprd+ neuron as in *A* evoked at −20 mV before (total I$_{Na+}$) and after (TTX-r I$_{Na+}$, TTX-resistant) application of 1 μM TTX. The TTX-s I$_{Na+}$ (TTX-sensitive) sweep was generated by digitally subtracting the TTX-r I$_{Na+}$ sweep from the total I$_{Na+}$ sweep. *C*: current-voltage relationship for the Mrgprd+ neuron detailed in *A* and *B*. Peak current amplitudes were taken before and after addition of TTX for Total I$_{Na+}$ (■) and TTX-r I$_{Na+}$ (●), respectively. The TTX-s I$_{Na+}$ (▲) was determined at each voltage using the same method as in *B*.
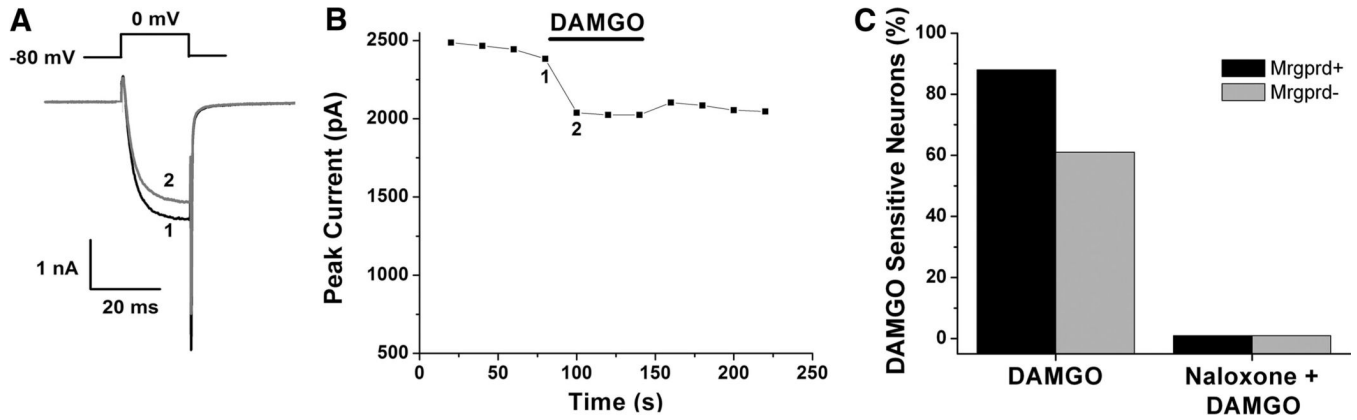
FIG. 3.

Mrgprd+ neurons display voltage-gated Ca^{2+} current that is negatively modulated by DAMGO. *A*: voltage-gated Ca^{2+} current in a representative Mrgprd+ neuron evoked at 0 mV from a holding potential of -80 mV before (*1*) and after (*2*) addition of 1 μM DAMGO. *B*: time course of peak Ca^{2+} current amplitude evoked every 20 s. DAMGO (1 μM) was applied for 60 s where indicated, and time points *1* and *2* correspond to the sweeps in *A*. *C*: a higher percentage of Mrgprd+ neurons (88%, $n = 25$) display sensitivity to DAMGO when compared with Mrgprd$-$ neurons (61%, $n = 18$). No inhibition of Ca^{2+} current was observed in either population when 10 μM naloxone was given for 20 s before and during DAMGO application ($n = 6$).
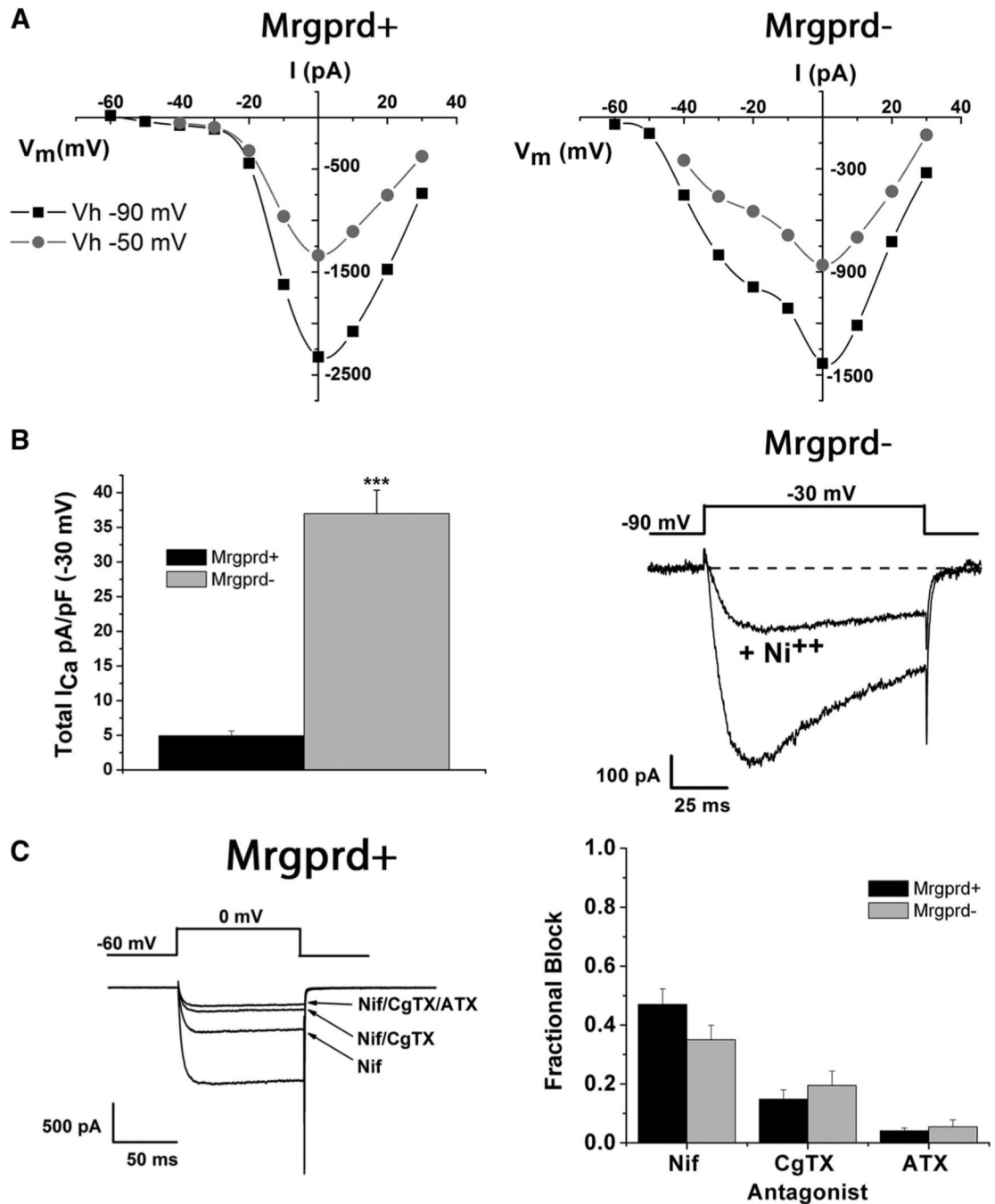
FIG. 4.

Mrgprd+ neurons display several types of voltage-gated Ca^{2+} current but do not display low-threshold Ca^{2+} current. *A*: current-voltage relationships for Mrgprd+ (*left*) and Mrgprd− (*right*) neurons. Ca^{2+} current was evoked every 20 s from a holding potential of either −90 mV (■) or −50 mV (○). Note the larger Ca^{2+} current amplitude in Mrgprd− neurons at voltages negative to −20 mV. *B*: total I_{Ca++} density (*left*) evoked from a holding potential of −90 mV to a test potential of −30 mV in Mrgprd+ (*n* = 13) and Mrgprd neurons (*n* = 12). The I_{Ca++} at −30 mV in a representative Mrgprd− - neuron (*right*) is sensitive to block by 100 μM Ni^{2+}. *C*: total I_{Ca++} in a representative Mrgprd+ neuron (*left*) evoked at 0 mV from a holding potential of −60 mV before and after addition of 30 μM nifedipine, 1 μM ω-conotoxin GVIA, and 250

nM ω-agatoxin IVA. Antagonists were applied for ≥60 s. The fraction of I_{Ca++} blocked by each antagonist (*right*) is shown for both Mrgprd+ (*n* = 10) and Mrgprd− (*n* = 10) neurons.
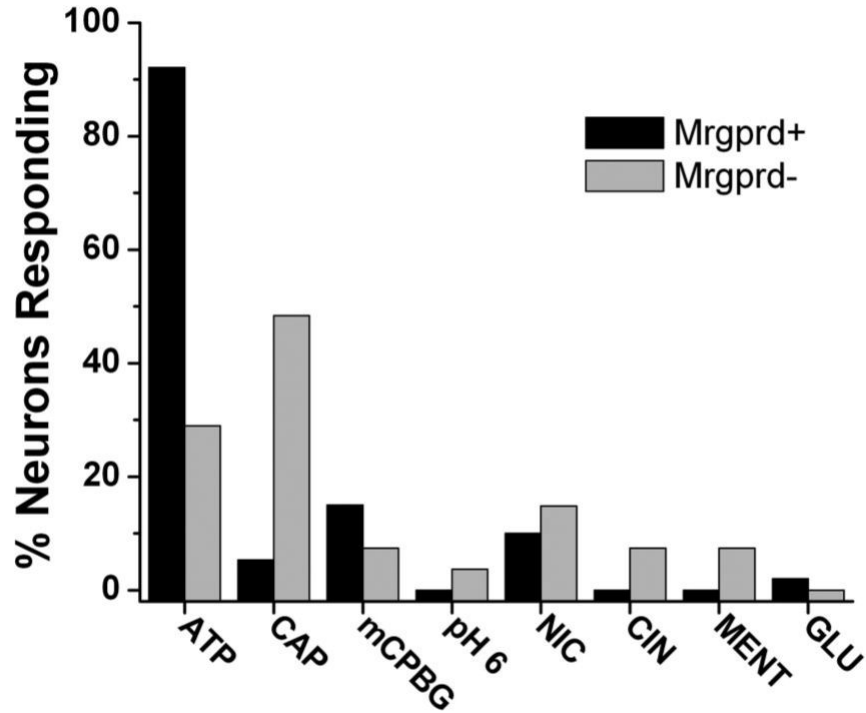
FIG. 5.
Mrgprd+ neurons respond predominantly to application of ATP. Concentrations of ligands applied were (in μM) 50 ATP, 2 CAP (capsaicin), 3 mCPBG (a 5-HT3 agonist), 500 NIC (nicotine), CIN (cinnamaldehyde) 100, MENT (menthol) 100, and GLU (glutamate) 1,000. Sample sizes were (listed as n = Mrgprd+, Mrgprd− for each ligand): ATP n = 40, 38; CAP n = 37, 39; mCPBG n = 21, 20; pH 6.0 n = 26, 23; NIC n = 22, 21; CIN n = 22, 25; MENT n = 24, 21; GLU n = 15, 15. An arbitrary cutoff of 50 pA was used to determine whether response was positive or negative.
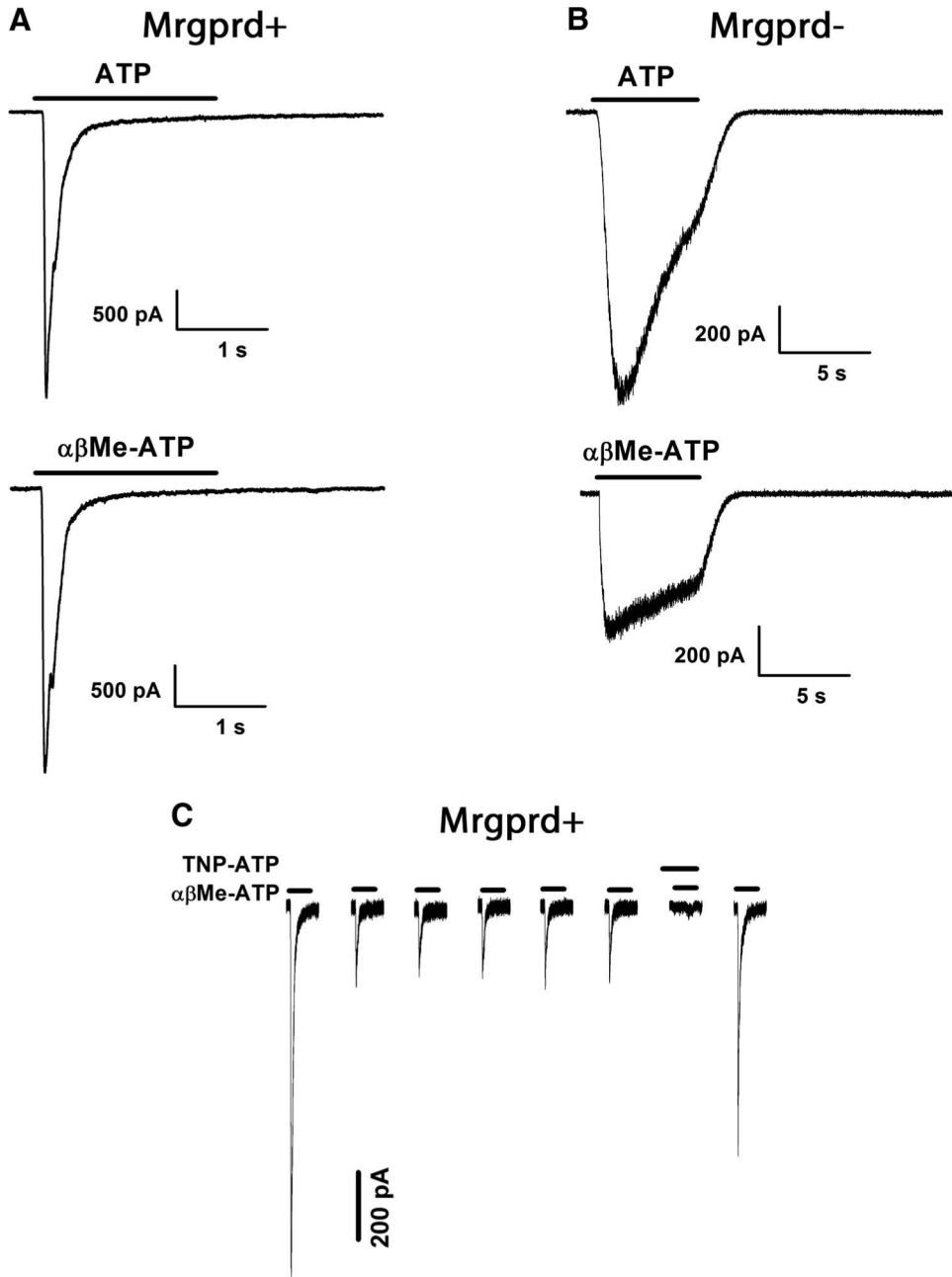
FIG. 6.
Mrgprd+ neurons display current kinetics and pharmacology consistent with expression of the P2X3 receptor. *A*: representative traces from separate Mrgprd+ neurons responding to either 50 μM ATP (*top*) or 50 μM $\alpha\beta$Me-ATP (*bottom*). *B*: representative traces from separate Mrgprd- neurons responding to either 50 μM ATP (*top*) or 50 μM $\alpha\beta$Me-ATP (*bottom*). Note the change in the horizontal time scale in. *C*: the current in Mrgprd+ neurons is blocked by 50 nM TNP-ATP. An application of 50 μM $\alpha\beta$Me-ATP was given for 1 s every 60 s (horizontal time between applications not to scale). TNP-ATP (50 nM) was applied for 10 s before and during the 7th application of $\alpha\beta$Me-ATP and then washed off. All recordings were made at −70 mV.

TABLE 1

Nociceptor-like properties of Mrgprd+ and Mrgprd− neurons

	Mrgprd+	*n*	Mrgprd−	*n*
Diameter, μm	20.1 ± 0.1	160	19.3 ± 0.3	184
Capacitance, pF	21.3 ± 0.4	178	17.2 ± 0.4	191
AP duration, ms	6.6 ± 0.3*	26	5.2 ± 0.5	20
AP amplitude, mV	112.5 ± 3.2*	26	104.2 ± 2.6	20
AP overshoot, mV	63.5 ± 2.3*	26	56.9 ± 1.9	20
Rest potential, mV	-48 ± 1	22	-46 ± 2	19
Input resistance, GΩ	1.4 ± 0.1	48	1.6 ± 0.1	43
TTX$_s$ I_{Na}, pA/pF	41.4 ± 5.9	24	52.7 ± 11.3	26
TTX$_r$ I_{Na}, pA/pF	188.8 ± 9.7**	24	132.8 ± 19.8	26

Cell body diameter was measured using a calibrated graticule. Statistical significance was determined using a two-tailed Student's *t*-test

*
$P < 0.05$

**
$P < 0.01$). AP, action potential.